Epoxy resin nanocomposites with hydroxyl (OH) and amino (NH2) functionalized boron nitride nanotubes

Guan, Jingwen; Ashrafi, Behnam; Martinez-Rubi, Yadienka; Jakubinek, Michael B.; Rahmat, Meysam; Kim, Keun Su; Simard, Benoit

Publisher's version / Version de l'éditeur:
https://doi.org/10.1080/20550324.2018.1457764
Nanocomposites, 4, 1, pp. 10-17, 2018-04-25

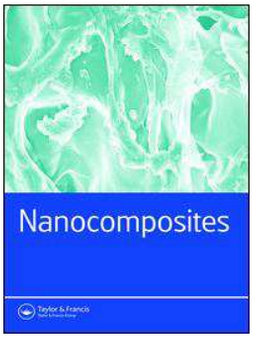

Nanocomposites

ISSN: 2055-0324 (Print) 2055-0332 (Online) Journal homepage: http://www.tandfonline.com/loi/ynan20

Epoxy resin nanocomposites with hydroxyl (OH) and amino (NH_2) functionalized boron nitride nanotubes

Jingwen Guan, Behnam Ashrafi, Yadienka Martinez-Rubi, Michael B. Jakubinek, Meysam Rahmat, Keun Su Kim & Benoit Simard

To cite this article: Jingwen Guan, Behnam Ashrafi, Yadienka Martinez-Rubi, Michael B. Jakubinek, Meysam Rahmat, Keun Su Kim & Benoit Simard (2018) Epoxy resin nanocomposites with hydroxyl (OH) and amino (NH_2) functionalized boron nitride nanotubes, Nanocomposites, 4:1, 10-17, DOI: 10.1080/20550324.2018.1457764

To link to this article: https://doi.org/10.1080/20550324.2018.1457764

NANOCOMPOSITES, 2018
VOL. 4, NO. 1, 10–17
https://doi.org/10.1080/20550324.2018.1457764

Taylor & Francis
Taylor & Francis Group

RESEARCH ARTICLE

Epoxy resin nanocomposites with hydroxyl (OH) and amino (NH_2) functionalized boron nitride nanotubes

Jingwen Guan[a], Behnam Ashrafi[b], Yadienka Martinez-Rubi[a], Michael B. Jakubinek[a], Meysam Rahmat[c], Keun Su Kim[a] and Benoit Simard[a]

[a]Security and Disruptive Technologies Research Centre, National Research Council Canada, Ottawa, Canada; [b]Aerospace Research Centre, National Research Council Canada, Montreal, Canada; [c]Aerospace Research Centre, National Research Council Canada, Ottawa, Canada

ABSTRACT

Hydroxyl (OH) and amino (NH_2) functionalized boron nitride nanotubes (f-BNNTs) were integrated into an epoxy resin (Epon828) to achieve improved mechanical properties. While raw BNNT-composites yielded the largest values for Young's modulus and appeared to be well mixed, f-BNNTs were found to provide a superior combination of mechanical properties yielding improvements in strain at failure, tensile strength and toughness that were not observed using raw BNNTs. In particular, an increase of 21% in Young's modulus is observed with 5 wt% of f-BNNT, and increases of 12, 21, and 49% are observed in tensile strength, failure strain, and toughness, respectively, with 2 wt% f-BNNT while a 34% increase in fracture toughness is observed with 3 wt% f-BNNT.

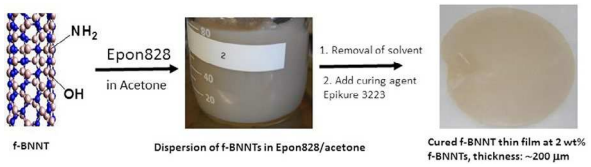

ARTICLE HISTORY
Received 25 January 2018
Accepted 22 March 2018

KEYWORDS
Boron nitride nanotubes (BNNTs); epoxy resin; nanocomposite; functionalization; mechanical properties

Introduction

Incorporation of nanofiller such as carbon nanotubes (CNTs) and boron nitride nanotubes (BNNTs) within polymer matrices can improve their mechanical performance along with adding multifunctional features like electrical and/or thermal conductivity. Great effort to harness the superlative properties of CNTs in composites has been made over the past two decades, showing interesting mechanical and conductivity improvements.[1–4] Generally, the primary factors limiting the overall performance improvement are the van der Waals interactions between nanotubes, which promote agglomeration (bundling), and the lack of interfacial interactions leading to limited load transfer between nanotubes and the matrix. These issues can be partially mitigated through chemical surface modifications.[5–8] BNNTs offer equally good mechanical properties to CNTs (e.g. Young's modulus of 1.2 TPa vs. 1.3 TPa for CNTs[9,10]) and while nanocomposites with BNNTs present similar integration challenges. Recent reports have demonstrated good interfacial interactions between BNNTs and polymers including easier wetting and higher interfacial shear strength.[11–14] This suggests that BNNTs may be superior for reinforcing epoxy than CNTs in some cases. In addition, BNNTs provide a range of different functional properties (e.g. Table 1) including considerably high thermal stability, wide band gap (~6 eV), high electrical resistivity and breakdown strength, high neutron absorption capability, and transparency in the visible light region. These offer advantages for certain applications such as transparent armor, aircraft windows, electrical insulation, and space structures.

Recent advances in synthesis and large-scale production of BNNTs[16,20–22] offer increased potential to explore BNNTs in polymer nanocomposites. Historically, BNNT polymer nanocomposites have received relatively limited studies[23] but improvements in mechanical and thermal properties have been reported.[24–27] Recently, we reported improvements in Young's modulus, fracture toughness, and single-lap-shear strength for an epoxy adhesive with raw (as-produced), unfunctionalized BNNTs (r-BNNT)[28]; however, tensile strengths were decreased. In addition to many examples in the CNT literature, nanotube functionalization has also

CONTACT Jingwen Guan Jingwen.guan@nrc-cnrc.gc.ca

Table 1. Comparison of properties of carbon nanotubes and boron nitride nanotubes

	Carbon nanotubes (CNTs)	Boron nitride nanotubes (BNNTs)	Refs.
Building block	C	B and N	
Mechanical property	Elastic modulus 1.3 TPa, Strength > 65 GPa	Elastic modulus 1.18 TPa	9, 10
Electrical conductivity	Metallic, ballistic conductor, ampacity > 10^9 A/cm^2 >> Cu; Semiconducting, bandgap about 0.5–2 eV	Large band gap (~6 eV), insulator	15–17
Thermal conductivity	>3000 Wm^{-1}K^{-1} at 25 °C, better than diamond	High, but lower than CNTs (minimal data)	16, 17
Optical properties	Absorb across the visible spectrum, NIR fluorescence	Transparent in visible and infrared region, absorb UV	16, 18, 19
Thermal stability	Stable up to 400 °C in air	Stable up to 900 °C in air	16
Neutron absorption cross section	C: 0.003 barns	B: 767 barns (^{10}B ~3800 barns); N: 1.9 barns	16
Visual appearance	Black in mixture of metallic and semiconducting	Snow white in pure form; beige/brown with common impurities	
Structure and dimension	Hollow core in one dimension, high aspect ratio	Hollow core in one dimension, high aspect ratio	

been shown to improve the nanoreinforcing effect of BNNTs.[29] In this work we employ hydroxyl (–OH) and amino (–NH_2) functionalized BNNTs (f-BNNT), generated via bromination and hydrolyzation reactions, to improve interaction with an epoxy matrix Epon828. The mechanical reinforcement effect of these functionalized BNNT–epoxy resin composites is compared to that of similar r-BNNT nanocomposites[28] as well as to similarly prepared CNT composites.

Materials and methods

Materials

A commercial epoxy resin (Epon828) and curing agent (Epikure 3223) were used in this study, and the portion of curing agent applied was twelve parts per hundred parts of resin (PPH) by weight based on the optimized mixing ratio recommended by the manufacturer.[30]

The r-BNNT material (Figure 1(a)) was manufactured from an h-BN powder feedstock through an RF induction thermal plasma process as reported previously.[20] The r-BNNTs contain a noticeable amount of impurities (Figure 1(b)) but have a high crystallinity, small diameters (~5 nm), lengths of ~1–5 μm and few walls (2–10 walls) for the majority of the BNNT population as shown in the transmission electron microscopy (TEM) images (Figure 1(c)). The impurities likely include untreated h-BN feedstock, newly generated BN phases (e.g. h-BN flakes, turbostratic BN, amorphous BN), organic BN compounds, polymeric BNs, and elemental boron particles/aggregates generated during the BNNT production process. The BNNT materials used for the composite preparations in this study were r-BNNTs without any treatment, and hydroxyl (–OH)/amino (–NH_2) functionalized BNNTs (denoted as f-BNNTs) with high purity. The amount of BNNTs is estimated to be >50 wt% and >80 wt% by scanning electron microscopy (SEM) in the r-BNNT (Figure 1(b)) and f-BNNT sample (Figure 2(a)), respectively. The chemistry and characterization of the combined purification and functionalization can be found elsewhere in detail.[31] In brief, r-BNNT material was washed in water with assistance of ultrasonication to remove non-tubular BN impurities, and then the enriched BNNTs together with enriched elemental boron aggregates were treated with liquid bromine in water. The non-encapsulated elemental boron particles were effectively removed by reacting with bromine forming soluble boric acid in water solution. Excess bromine reacts also with the outer layer of BNNTs. This results in functionalization of BNNTs by B-N bond cleavage through bromination and hydrolyzation *in situ*.[31] For comparison, industrial grade CNTs (NC7000™) and research grade CNT-COOHs (NC3101™) were purchased from Nanocyl SA (Belgium) and used as received.

Nanocomposite preparation

The r-BNNT composites were prepared from r-BNNT powder (dried at 120 °C overnight) that was mixed with Epon828 by planetary centrifugal mixing (Thinky ARE 310).[28] For comparison, CNT-Epon828 and CNT-COOH-Epon828 were prepared in the same dry mixing procedures.

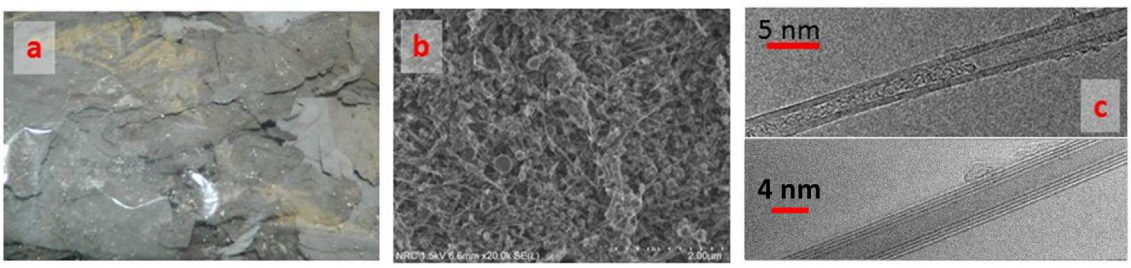

Figure 1. Raw BNNTs: (a) photograph of bulky mass in a plastic bag, (b) SEM image of r-BNNTs, (c) TEM images of individual BNNTs.

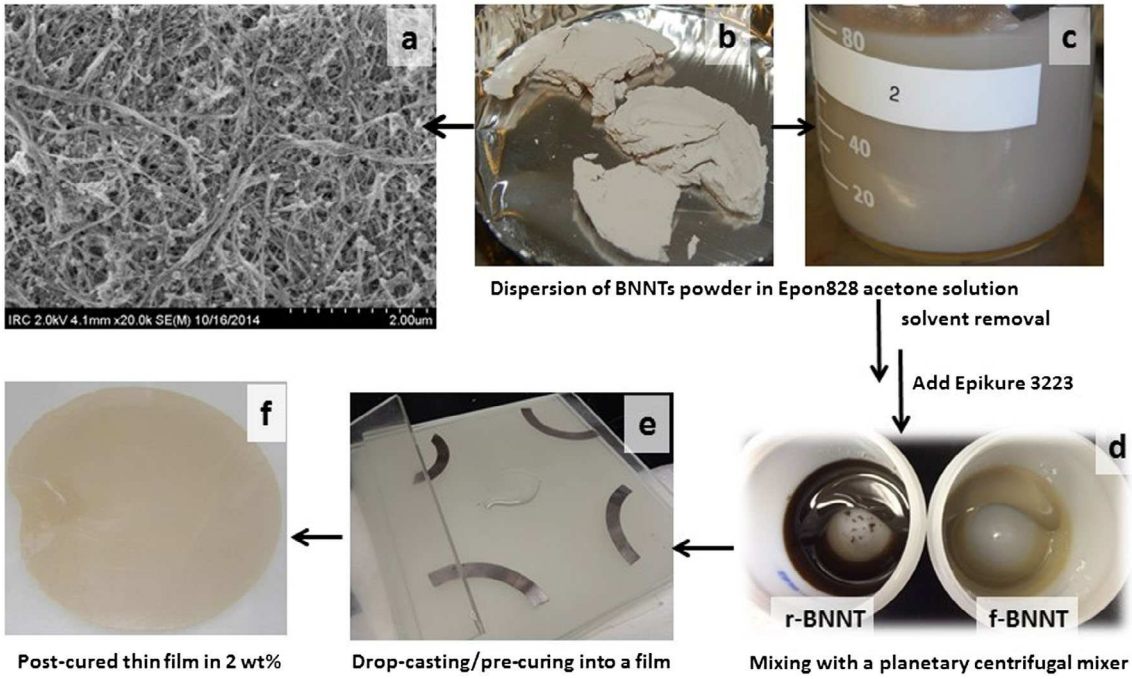

Figure 2. Functionalized BNNTs: (a) SEM image from the dry material shown in (b), (b) photograph of the dry functionalized BNNT material used along with photographs from the composite preparation via (c) solvent processing in acetone followed by solvent removal in vacuum, (d) planetary mixing of the hardener, (e) casting and curing of BNNT epoxy composite and (f) post-cured thin film (~200 μm in thickness) that has a relatively good transparency comparing with a similar CNT composite film.

In a typical experimental procedure for f-BNNT composite with a 3 wt% content, 834 mg of f-BNNTs (Figure 2(b)) were dispersed in ~175 ml of acetone (Figure 2(c)). The dry f-BNNTs were first ground into a fine powder with a small amount of acetone in an agate mortar and then placed into a capped bottle with additional acetone solvent. The mixture was bath-sonicated for 30 min at a time, and repeating sonication cycles were applied until a well-dispersed suspension formed. To this f-BNNT-dispersion in acetone, a small portion (~5 g) of the total amount (26.9 g) of Epon828 was added and the mixture was magnetically stirred to passivate the f-BNNT surface in a diluted epoxy resin environment in order to achieve a good dispersion with the aid of the dissolved epoxy resin. The mixture was continuously stirred overnight at room temperature and then bath-sonicated for 30 min. Finally, the remaining epoxy resin was added into the mixture and the mixture was stirred for an additional 6 h at room temperature plus 30 min bath-sonication followed by a 3 h stirring at 60 °C. Afterward, the acetone solvent was vaporized with a nitrogen flow under stirring at 60 °C. The residue was dried in a vacuum oven at 80 °C for 8 h to further remove any residual solvent and then cooled to room temperature under nitrogen.

Curing procedure

The BNNT–epoxy resin composites, after solvent removal where applicable, were mixed with the curing agent (Epikure 3223) at 12 parts curing agent per hundred parts resin (by weight) using a planetary centrifugal mixer (Thinky ARE 310) as shown in Figure 2(d), for 1 min at 2000 rpm followed by degassing at 2200 rpm for 30 s. The well-mixed liquid sample was cast onto a glass plate treated with a release agent (Frekote 770-NC, part No. 83469). A second glass plate was used to compress the resin and a 200 μm metal shim was placed between the two plates to control the film thickness. Once the top glass plate was carefully and slowly laid down (to minimize trapping of air bubbles) a heavy block, sufficient to compress the sample to the thickness of the metal shims, was placed on top of the glass plate. The sample was kept at room temperature for 48 h to cure, after which it was post-cured in a convection oven at 120 °C for 2 h. After cooling to room temperature, the thin film samples were easily removed from the glass plates (Figure 2(f)). Neat Epon828 and CNT-composites were cured under the same conditions.

Tensile characterization

A micro-tensile test frame (Fullam Substage Test Frame) was used to measure the mechanical properties of the fabricated thin films. At least five dogbone specimens, according to ISO 527-2 (Type 1BB), were punched out from each thin film sample and tested. For all tests a displacement rate of 1 mm/min and a load cell of 50 N were used.

Fracture toughness characterization

Plane-strain fracture toughness (K_{IC}) was measured using five rectangular specimens of 2 × 4 × 20 mm

according to ASTM D-5045. A precision saw was used to create a notch of ~1 × 2 mm on samples and the notch was then sharpened with a fresh razorblade. The same micro-tensile test frame (Fullam Substage Test Frame) was used to perform a 3-point fracture toughness test at a displacement rate of 3 mm/min.

Scanning electron microscopy and transmission electron microscopy measurements

The SEM images of BNNTs were taken using a Hitachi S-4800 field emission scanning electron microscope. All images were a combination of secondary and back-scattered electrons captured using PCI Quartz SEM imaging software. The high-resolution TEM images were acquired at 300 kV at NRC and at 80 kV at the Canadian Centre for Electron Microscopy at McMaster University. Imaging samples were prepared by placing a few drops of a suspension of BNNTs in methanol or in water onto an aluminum stub for SEM measurement and onto a holey carbon film coated Cu grid for TEM.

Results and discussion

Figure 3 summarizes the Young's modulus and tensile strength of the BNNT–epoxy nanocomposites. Young's modulus of both r-BNNT and f-BNNT composites were higher than the neat epoxy resin and increased with BNNT content. We observe these significant improvements in Young's modulus, relative to the neat epoxy matrix, even by simple solvent-free mixing of r-BNNTs (25% at 2 wt% r-BNNTs).[28] This, along with the continued trend to relatively high loadings, indicates that an effective dispersion of r-BNNTs in the epoxy matrix has achieved.

While r-BNNT addition improved the Young's modulus, as well as fracture toughness and lap-shear-strength, the tensile strength was not improved and actually decreased slightly (within the error limits) with any r-BNNT addition evaluated.[28] Conversely, here we observed that the tensile strength improved with f-BNNT addition (Figure 3, e.g. +12% with 2 wt% f-BNNT). The

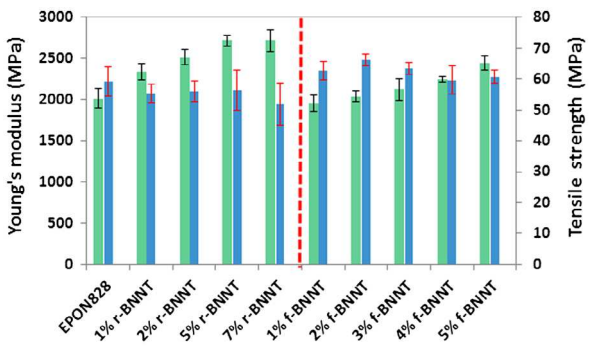

Figure 3. Comparison of Young's modulus (green bars) and tensile strength (blue bars) among neat Epon828, r-BNNT composite (1–7 wt%,[28]), and f-BNNT composites (1–5 wt%).

change in tensile strength is qualitatively different from the trend seen with r-BNNTs and suggests effective binding between OH/NH_2 groups and the epoxy matrix, which could be in the form of covalent connections or hydrogen bonds. Both types of samples do not have the same trend of tensile strength with the tube content, although both groups show a decrease beyond 2 wt%. This may suggest that the functionalized BNNTs may not disperse as effectively as the raw BNNTs, which mainly exist as individual tubes and smaller bundles, while purification always result in larger bundles of BNNTs. Therefore, surface functionalization leads to exfoliation and better interactions with the matrix if proper functional groups have been chosen, as in the case here. As shown in Figure 3, the enhancement of the Young's modulus with these f-BNNTs is not as high as with r-BNNT but the trend is similar. In order to better understand the trend in Young's modulus, a dimensionless parameter for reinforcement efficiency (e) is introduced:

$$e = \frac{(E_c - E_m)}{E_m V_f},$$

where E_c and E_m are composite and polymer Young's modulus, respectively, and V_f is volume fraction of fibers. A higher e corresponds to a higher efficiency of fiber reinforcement. A wide range of reinforcement efficiencies (commonly in the range of 1–60[32]) are observed in the CNT literature. At low content of r-BNNTs (<1 vol %, where 1 wt% ~0.63 vol % BNNTs), e is ~25 in this study. This efficiency is reduced to less than 6 for higher r-BNNT content (~4 vol %), which can be attributed primarily to the agglomeration of r-BNNTs at higher contents. The parameter e is generally lower for f-BNNTs than for r-BNNTs. This could be explained by damage introduced to f-BNNTs (e.g. shortening of the length of f-BNNTs as well as damage to wall due to the chemical modification and sonication steps). It has been well documented in the case of CNTs that the nanotube length significantly drops in liquid media with increasing sonication time, power and temperature through a scission mechanism.[33–41] In contrast to the case for r-BNNTs, the e increases as the f-BNNT content increases from 1 to 5 wt%. This suggests that the addition of higher contents of BNNTs does not cause as much agglomeration in the f-BNNT case, as expected due to functionalization. Additionally, the solution process employed for f-BNNTs may also result in less agglomeration at higher BNNT content.

The enhancement of the Young's modulus is also compared to Halpin–Tsai model[32,42] for randomly oriented fibers. In this model, the composite Young's modulus is given by:

$$E_c/E_m = \frac{3}{8}\left(\frac{1 + 2s\eta_L V_f}{1 - \eta_L V_f}\right) + \frac{3}{8}\left(\frac{1 + 2\eta_T V_f}{1 - \eta_T V_f}\right),$$

where s is the fiber aspect ratio (length divided by diameter). Also, η_L and η_T are given by:

$$\eta_L = \frac{E_f/E_m - 1}{E_f/E_m + 2s} \text{ and } \eta_T = \frac{E_f/E_m - 1}{E_f/E_m + 2},$$

where E_f is fiber Young's modulus.

For, an illustrative BNNT with Young's modulus and aspect ratio of ~600 GPa and ~200, respectively, and an epoxy Young's modulus of 2 GPa, this leads to a theoretical reinforcement efficiency of ~66. The highest reinforcement efficiency observed here, e = 25 for low content of r-BNNTs, is still less than half of this predicted value and the efficiency falls over 1 order of magnitude for the case of f-BNNTs. However, this large gap between the Halpin–Tsai model prediction and the experiment results is consistent with studies published on CNT-based polymer composites.[32] The Halpin–Tsai model considers a perfect load transfer between fiber and resin. A combination of low polymer–nanotube interaction, agglomeration of BNNTs, formation of BNNT bundles (leading to a lower effective aspect ratio for BNNTs), and the existence of impurities in the BNNT samples (leading to lower actual content of BNNTs) can explain this large gap between the experimental results and the Halpin–Tsai model prediction.

Figure 4 illustrates the failure strain and tensile toughness for the r-BNNT and f-BNNT composites. With r-BNNT, the tensile toughness decreased continuously with increasing nanotube content from 1 to 7 wt%. Conversely, with f-BNNT, the composites generally have higher tensile toughness, with improvements relative to the neat epoxy of up to ~50% with 2 wt% f-BNNT content, and comparable tensile toughness to that of the neat epoxy even at the highest f-BNNT content of 5 wt%. These differences in toughness follow the differences in failure strain, and the improved performance of the f-BNNT composites follows from their ability to withstand higher strain. The composite with 2 wt% f-BNNT content had the highest strain at break, an increase of over 20% relative to the neat Epon828. The modulus of resilience, which is also a measure of energy absorption – the amount that is absorbed elastically before permanent deformation – is increased for nearly all of the BNNT composites with either r- or f-BNNT. The greatest improvement with r-BNNTs is about 112%, and for each sample from 1 to 5 wt%, the increase is considerably impressive. The 5 wt% addition of r-BNNTs increased both Young's modulus and tensile stress at yield, which lead to the significant increase in the modulus of resilience, while tensile toughness decreased due to the limited strain. Interestingly, the intermediate-loading (2–3 wt%) f-BNNT composites also showed increased modulus of resilience despite the much smaller increase in Young's modulus. For f-BNNT composites, the modulus of resilience follows the tensile toughness, in direct contrast to the case with the higher stiffness with r-BNNTs.

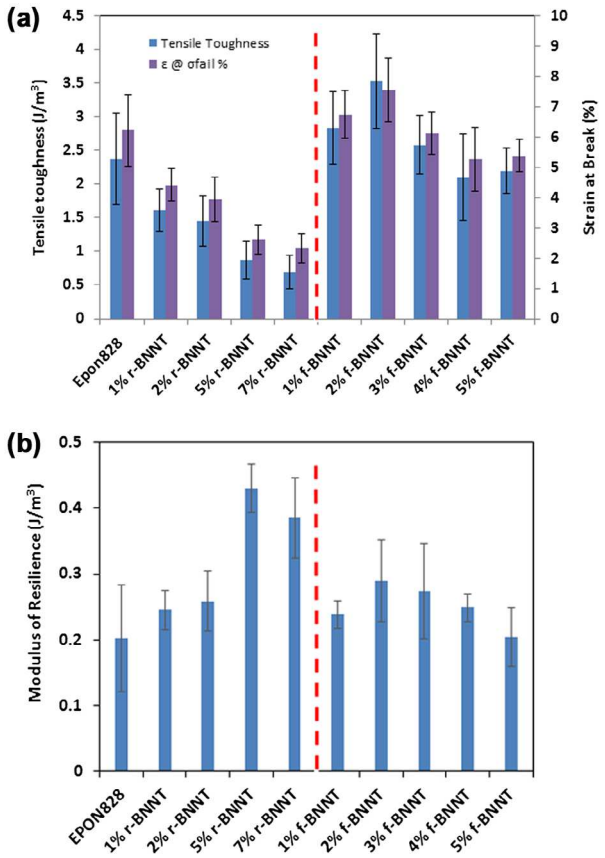

Figure 4. Comparison of (a: top) tensile toughness (blue bars) and failure strain (purple bars), and (b: bottom) modulus of resilience, between neat Epon828, r-BNNT composites (1–7 wt%), and f-BNNT composites (1–5 wt%).

The fracture toughness was similarly improved with f-BNNTs as was observed with r-BNNTs (Figure 5). While for some mechanical properties (e.g. Young's modulus and modulus of resilience) the greatest increase is obtained with the highest contents of r-BNNTs, high

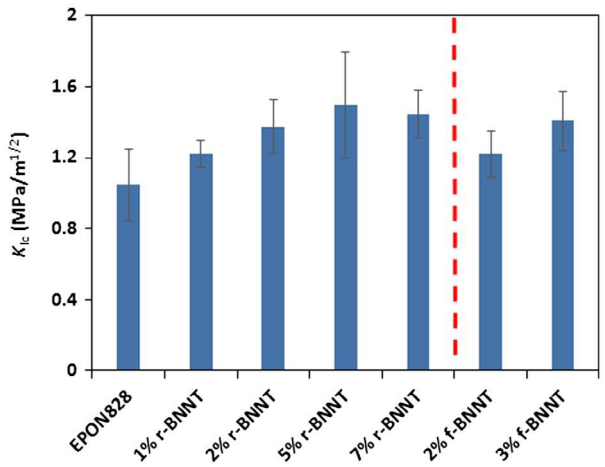

Figure 5. Comparison of fracture toughness (K_{Ic}) among neat Epon828, r-BNNT composites[28], and f-BNNT composites.

Table 2. Comparison of mechanical properties of neat Epon828 with BNNT–epoxy and CNT–epoxy composites at 2 wt% nanotube content.

	Tensile stress @ Max load (MPa)	Tensile strain @ Max load (%)	Young's modulus (MPa)	Tensile stress @Yield (0.2% offset), (MPa)	Tensile strain @ break (%)	Tensile stress @ break (MPa)	K_{Ic} (MPa/m$^{0.5}$)
Neat Epon828	59 (5)	6.3 (1.3)	2015 (124)	27.6 (4.2)	6.2 (1.2)	59 (5)	1.05 (0.20)
2% r-BNNT	56 (3)	3.9 (0.7)	2514 (88)	36 (3)	3.9 (0.7)	56 (3)	1.37 (0.15)
% diff.	−5	−38	+25	+30	−37	−5	+30
2% f-BNNT	66 (2)	7.5 (1.1)	2040 (61)	34 (3)	7.5 (1)	66 (2)	1.22 (0.13)
% diff.	+12	+19	+1.2	+26	+21	+12	+15
2% CNT	43 (8)	3.3 (0.8)	1897 (101)	27.3 (1.6)	3.3 (0.9)	43 (8)	1.12 (0.07)
% diff.	−27	−48	−6	−1	−47	−27	+7
2% CNT-COOH	45 (12)	4.0 (1.6)	1794 (67)	26.0 (0.3)	4.0 (1.7)	45 (13)	*
% diff.	−24	−36	−11	−6	−35	−24	

Notes: Numbers in brackets indicate the standard deviation of multiple measurements, and the percentage differences (% diff) are calculated with respect to the neat Epon828 sample. *The value is not measured.

r-BNNT content is disadvantageous for strength as well as processing considerations (e.g. ease-of-dispersion, quantity of nanomaterial). In comparison, the 2–3 wt% f-BNNT composites demonstrate increased Young's modulus, modulus of resilience, and fracture toughness, along with superior improvements in tensile strength, strain at failure, and tensile toughness. This is because the f-BNNT offer improved interfacial interaction with the matrix due to the OH or NH_2 groups and reduced level of impurities. Our data suggest that 2–3 wt% of these f-BNNTs provides an optimal composition range for enhancement of mechanical properties.

In comparison to the r-BNNT and f-BNNT composites, CNT–Epon828 composites (Table 2) did not demonstrate any improvement except in fracture toughness. This may indicate that poor wettability of the CNTs in the dry mixing process compared to the BNNTs resulted in severe agglomeration.

Conclusions

Hydroxyl- and amino-functionalized BNNT epoxy nanocomposites demonstrate consistently positive improvements over the baseline epoxy and corresponding composites with r-BNNTs in Young's modulus, tensile strength, failure strain, tensile toughness, and fracture toughness, suggesting that the surface functional OH/NH_2 groups have significant interactions and/or covalent connections with epoxide groups thus offering better load transfer and interfacial compatibility. The range of 2–3 wt% f-BNNT content provides an optimal composition for a significant reinforcement of mechanical properties.

Acknowledgements

The authors acknowledge the nanotube production team at the NRC's facility and express thanks to Gordon Chan (NRC) for the SEM measurements, Martin Couillard (NRC) and Xiaomei Du (NRC) as well as Andreas Korinek and Gianluigi Botton at the Canadian Centre for Electron Microscopy at McMaster University for the TEM measurements. Funding to support synthesis of BNNTs and development of BNNT nanocomposites was provided by the National Research Council Canada through the Security Materials Technology Program. The paper is developed based on the presentation (1205-1/nano-composite 2, proceeding number: 3527) at the 21st International Conference on Composite Materials (ICCM21), Xi'an, China, 20–25 August 2017.

Disclosure statement

No potential conflict of interest was reported by the authors.

Funding

This work is supported by the Security Materials Technology Program of the National Research Council Canada.

ORCID

Jingwen Guan http://orcid.org/0000-0003-1759-2172

References

1 B. Ashrafi, J. W. Guan, V. Mirijalili, Y. Zhang, C. Li, P. Hubert, B. Simard, C. T. Kingston, O. Bourne and A. Johnston: 'Enhancement of mechanical performance of epoxy/carbon fibres laminate composites using single-walled carbon nanotubes', *Compos. Sci. Technol.*, 2011, **71**, (13), 1569–1598.
2 M. Rahmat and P. Hubert: 'Carbon nanotube-polymer interactions in nanocomposites: a review', *Compos. Sci. Technol.*, 2011, **72**, (1), 72–84.
3 Q. Zhang, J. Q. Huang, W. Z. Qian, Y. Y. Zhang and F. Wei: 'The road for nanomaterials industry: a review of carbon nanotube production, post-treatment, and bulk applications for composites and energy storage', *Small*, 2013, **9**, (8), 1237–1265.
4 M. Cl McCrary-Dennis and Ol I. Okoli: 'A review of multiscale composites manufacturing and challenges', *J. Reinf. Plast. Compos.*, 2012, **31**, (24), 1687–1711.
5 J. W. Guan, B. Ashrafi, Y. Martinez-Rubi, Y. Zhang, C. T. Kingston, A. Johnston and B. Simard: 'Integration of single-walled carbon nanotubes into a single component epoxy resin and an industrial epoxy resin system', *Polym. Polym. Compos.*, 2011, **19**, (2&3), 99–106.
6 B. Ashrafi, J. W. Guan, V. Mirijalili, P. Hubert, B. Simard and A. Johnston: 'Correlation between Young's modulus and impregnation quality of epoxy-impregnated SWCNT buckypaper', *Compos. Part A: Appl. Sci. Manuf.*, 2010, **41**, (90), 1184–1191.

7 Y. Martinez-Rubi, B. Ashrafi, J. W. Guan, C. T. Kingston, A. Johnston, B. Simard, V. Mirijalili, P. Hubert, L. Deng and R. Young: 'Toughening of epoxy matrices with reduced single-walled carbon nanotubes', *ACS Appl. Mater. Interfaces*, 2011, **3**, 2309–2317.

8 E. Najafi, J. Wang, A. P. Hitchcock, J. W. Guan, S. Dénommée and B. Simard: 'Characterization of single-walled carbon nanotubes by scanning transmission X-ray spectromicroscopy: purification, order and dodecyl functionalization', *J. Am. Chem. Soc.*, 2010, **132**, 9020–9029.

9 R. S. Ruoff, D. Qian and W. K. Liu: 'Mechanical properties of carbon nanotubes: theoretical predictions and experimental measurements', *C. R. Physique*, 2003, **4**, 993–1008 and references therein.

10 X. Chen, C. M. Dmuchowski, C. Park, C. C. Fay and C. Ke: 'Quantitative characterization of structural and mechanical properties of BNNTs in high temperature environments', *Nature*, 2017, DOI: 10.1038/s41598-017-11795-8. and references therein.

11 A. T. Nasrabadi and M. Foroutan: 'Interaction between polymers and single-walled boron nitride nanotubes: a molecular dynamics simulation approach', *J. Phys. Chem. B.*, 2010, **114**, 15420–15436.

12 S. Rouhi: 'Molecular dynamics simulation of the adsorption of polymer chains on CNTs, BNNTs and GaNNTs', *Fibers Polym.*, 2016, **17**, (3), 333–342.

13 K. S. Kim, M. B. Jakubinek, Y. Martinez-Rubi, B. Ashrafi, J. W. Guan, K. O'Neill, M. Plunkett, A. Hrdina, S. Lin, S. Dénommée, C. T. Kingston and B. Simard: 'Polymer nanocomposites from free-standing macroscopic boron nitride nanotube assemblies', *RSC Adv.*, 2015, **5**, 41186–41192.

14 X. Chen, L. Zhang, C. Park, C. C. Fay, X. Wang and C. Ke: 'Mechanical strength of boron nitride nanotube-polymer interfaces', *Appl. Phys. Lett.*, 2015, **107**, 253105.

15 T. W. Ebbesen, H. J. Lezec, H. Hiura, J. W. Bennett, H. F. Ghaemi and T. Thio: 'Electrical conductivity of individual carbon nanotubes', *Nature*, 1996, **382**, 54–56.

16 K. S. Kim, M. J. Kim, C. Park, C. C. Fay, S. Chu, C. T. Kingston and B. Simard: 'Scalable manufacturing of boron nitride nanotubes and their assemblies: a review', *Semicond. Sci. Technol.*, 2017, **32**, 013003 (18 pp).

17 B. E. Belkerk, A. Achour, D. Zhang, S. Sahli, M. Djouadi and Y. K. Yap: 'Thermal conductivity of vertically aligned boron nitride nanotubes', *Appl. Phys. Exp.*, 2016, **9**, 075002 (4 pp) and references therein.

18 S. K. Jain and P. Srivastava: 'optical properties of hexagonal boron nanotubes by first-principles calculations', *J. Appl. Phys.*, 2013, **114**, 073514 (10pp).

19 D. Golberg, Y. Bando, Y. Huang, T. Terao, M. Mitome, C. Tang and C. Zhi: 'Boron nitride nanotubes and nanosheets', *ACS Nano*, 2010, **4**, (6), 2979–2999.

20 (a) K. S. Kim, Ch. T. Kingston and B. Simard: 'Boron nitride nanotubes and process for production thereof', PCT WO2014/169382;(b) K. S. Kim, C. T. Kingston, A. Hrdina, M. B. Jakubinek, J. W. Guan, M. Plunkett and B. Simard: 'Hydrogen-catalyzed, pilot-scale production of small-diameter boron nitride nanotubes and their macroscopic assemblies', *ACS Nano*, 2014, **8**, (6), 6211–6220.

21 M. W. Smith, K. C. Jordan, C. Park, J. W. Kim, P. T. Lillehei, R. Crooks and J. S. Harrison: 'Very long single- and few-walled boron nitride nanotubes via the pressurized vapour/condenser method', *Nanotechnology*, 2009, **20**, 505604 (6 pp).

22 A. Fathalizadeh, T. Pham, W. Mickelson and A. Zettl: 'Scaled synthesis of boron nitride nanotubes, nanoribbons, and nanocomcoons using direct feedstock injection into an extended pressure, inductively-coupled thermal plasma', *Nano Lett.*, 2014, **14**, 4881–4886.

23 W. Meng, Y. Huang, Y. Fu, Z. Wang and C. Zhi: 'Polymer composites of boron nitride nanotubes and nanosheets', *J. Mater. Chem.*, 2014, **C2**, 10049–10061.

24 N. O. Bansal, J. B. Hurst and S. R. Choi: 'Boron nitride nanotube-reinforced glass composites', *J. Am. Ceram. Soc.*, 2006, **89**, (1), 388–390.

25 C. Y. Zhi: 'Boron nitride nanotube/polystyrene composites', *JSM Nanotechnol. Nanomed.*, 2013, **1**, (1), 1005.

26 M. B. Jakubinek, J. F. Niven, M. B. Johnson, B. Ashrafi, K. S. Kim, B. Simard and M. A. White: 'Thermal conductivity of bulk boron nitride nanotube sheets and their epoxy-impregnated composites', *Phys. Status Solidi A*, 2016, **213**, (8), 2237–2242.

27 X. L. Zeng, J. J. Sun, Y. M. Yao, R. Sun, J. B. Xu and C. P. Wong: 'A combination of boron nitride nanotubes and cellulose nanofibers for the preparation of a nanocomposite with high thermal conductivity', *ACS Nano*, 2017, **11**, 5167–5178.

28 M. B. Jakubinek, B. Ashrafi, Y. Martinez-Rubi, M. Rahmat, M. Yourdkhani, K. S. Kim, K. Laqua, A. Yousefpour, B. Simard: 'Nanoreinforced epoxy and adhesive joints incorporating boron nitride nanotubes', *Int. J. Adhes. Adhes.*, 2018, doi:10.1016/j.ijadhadh.2018.03.008.

29 S. Lin, B. Ashrafi, K. Laqua, K. S. Kim and B. Simard: 'Covalent derivatization of boron nitride nanotubes with peroxides and their application in polycarbonate composites', *New J. Chem.*, 2017, **41**, 7571–7577.

30 www.hexion.com/Products/ShowTechnicalDataSheet.aspx?id=3942&Rev=7/16/2012.

31 J. W. Guan and B. Simard: 'Modified BNNTs and solution thereof', US provisional patent application, filed on October 27, 2017, 62/1578003;J. W. Guan, K. S. Kim and B. Simard: 'Purification, functionalization and solution of BNNTs', *Chem. Commun*, in preparing.

32 J. N. Coleman, U. Khan, W. J. Blau and Y. K. Gun'ko: 'Small but strong: a review of the mechanical properties of carbon nanotube-polymer composites', *Carbon*, 2006, **44**, 1624–1652.

33 S. Jeong, O. Lee and K. Lee: 'Preparation of aligned carbon nanotubes with prescribed dimensions: template synthesis and sonication cutting approach', *Chem. Mater.*, 2002, **14**, 1859–1862.

34 H. B. Chew, M. W. Moon, K. R. Lee and K. S. Kim: 'Compressive dynamic scission of carbon nanotubes under sonication: fracture by atomic ejection', *Proc. R. Soc. A*, 2010, **0495**, 1–20.

35 P. Vichchulada, M. A. Cauble, E. A. Abdi, E. I. Obi, Q. Zhang and M. D. Lay: 'Sonication power for length control of single-walled carbon nanotubes in aqueous suspensions used for 2-dimensional network formation', *J. Phys. Chem. C*, 2010, **114**, 12490–12495.

36 S. Mouri, Y. Miyauchi and K. Matsuda: 'Dispersion-process effects on the photoluminescence quantum yields of single-walled carbon nanotubes dispersed using aromatic polymers', *J. Phys. Chem. C*, 2012, **116**, 10282–10286.

37 G. Pagani, M. J. Green, P. Poulin and M. Pasquali: 'Competing mechanisms and scaling laws for carbon nanotube scission by ultrasonication', *PNAS*, 2012, **109**, (29), 11599–11604.

38 M. D. Rosesell, C. Kuebel, G. Ilari, F. Rechberger, F. J. Heiligtag, M. Niederberger, D. Koziej and R. Erni: 'Impact of sonication pretreatment on carbon nanotubes: a transmission electron microscopy study', *Carbon*, 2013, **61**, 404–411.
39 E. J. Weydemeyer, A. J. Sawdon and C. Peng: 'Controlled cutting and hydroxyl functionalization of carbon nanotubes through autoclaving and sonication in hydrogen peroxide', *Chem. Commun.*, 2015, **51**, 5939–5942.
40 S. M. Sabet, H. Mahfuz, J. Hashemi, M. Nezakat and J. A. Szpunar: 'Effects of sonication energy on the dispersion of carbon nanotubes in a vinyl ester matrix and associated thermos-mechanical properties', *J. Mater. Sci.*, 2015, **50**, 4729–4740.
41 M. Ji, B. Daniels, A. Shieh, D. A. Modarelli and J. R. Parquette: 'Controlling the length of self-assembled nanotubes by sonication followed by polymer wrapping', *Chem. Commun.*, 2017, **53**, 12806–12809.
42 J. C. Halpin and J. L. Kardos: 'The Halpin-Tsai equations: a review', *Polym. Eng. Sci.*, 1976, **16**, (5), 344–352.